






Original Research

# Herkinorin Promotes $\mu$ -Opioid Receptor Internalization and Protects iPSC-Derived Neurons from Hypoxic/Ischemic Injury

Zhihai Ju<sup>1</sup> , Guyan Wang<sup>1</sup> , Yanhong Yan<sup>1</sup> , Xuan Liang<sup>1</sup> , Xu Cui<sup>1,\*</sup> 

<sup>1</sup>Department of Anesthesiology, Beijing Tongren Hospital, Capital Medical University, 100730 Beijing, China

\*Correspondence: [cuiyubjtr@ccmu.edu.cn](mailto:cuiyubjtr@ccmu.edu.cn) (Xu Cui)

Academic Editor: Bettina Platt

Submitted: 8 June 2025 Revised: 13 September 2025 Accepted: 16 September 2025 Published: 29 October 2025

## Abstract

**Background:** Hypoxic/ischemic brain injury remains a major clinical challenge, yet the cellular mechanisms linking oxygen-glucose deprivation/reperfusion (OGD/R) to opioid receptor regulation in human neurons are still not fully understood. The trafficking of  $\mu$ -opioid receptors (MOR) and  $\kappa$ -opioid receptors (KOR) is a key regulator of neuronal survival under stress. Most studies to date in this field have employed rodent models. However, given the molecular and physiological differences between rodents and humans, this study employed human induced pluripotent stem cell (iPSC)-derived neurons to investigate opioid receptor trafficking during OGD/R, as well as the neuroprotective effects of Herkinorin. **Methods:** Human iPSC-derived neurons were subjected to 2 h of OGD followed by 24 h of reoxygenation. Cells were treated with Herkinorin (0.1, 0.5, or 1  $\mu$ M) during OGD/R. Apoptosis was assessed using flow cytometry, while the localization of MOR and KOR in membrane and cytoplasmic fractions was analyzed using western blotting. Western blotting was also used to quantify the expression of apoptosis-related proteins Bcl-2-associated X protein (Bax), B-cell lymphoma 2 (Bcl-2), and cleaved Caspase-3. Statistical comparisons were performed using one-way ANOVA with Tukey's post hoc test or non-parametric equivalents. **Results:** OGD/R significantly increased neuronal apoptosis, upregulated pro-apoptotic Bax and cleaved Caspase-3, and downregulated anti-apoptotic Bcl-2. These changes were accompanied by altered distribution of MOR, but not KOR localization, specifically decreasing cytoplasmic MOR while maintaining membrane levels. Herkinorin, particularly at 1  $\mu$ M, induced redistribution of MOR from the plasma membrane to cytoplasm, consistent with receptor internalization; it also significantly reduced apoptosis in a concentration-dependent manner. Furthermore, treatment with Herkinorin reversed the OGD/R-induced molecular changes by decreasing the expression of Bax and cleaved Caspase-3, while increasing that of Bcl-2. KOR trafficking remained largely unchanged under all conditions. Importantly, Herkinorin concentrations above 10  $\mu$ M reduced neuronal viability, indicating a narrow therapeutic window. **Conclusions:** Herkinorin exerts neuroprotective effects in human iPSC-derived neurons subjected to OGD/R, potentially by modulating MOR internalization and influencing mitochondrial-dependent apoptotic pathways. However, its efficacy is restricted to a limited dose range (0.1–1  $\mu$ M), as higher concentrations are toxic. The receptor subtype-specific trafficking pattern observed in this study underscores the importance of human-relevant models for mechanistic and translational research on opioid receptors.

**Keywords:** brain ischemia; opioid receptors,  $\mu$ ; opioid receptors,  $\kappa$ ; receptor internalization; induced pluripotent stem cells; neuroprotection; apoptosis; Herkinorin

## 1. Introduction

Hypoxic/ischemic brain injury is a major cause of long-term neurological disability and mortality, with few effective therapies available. A persistent barrier to the development of treatments is the low success rate for translation of findings from preclinical studies to clinical therapies. While rodent models have provided valuable mechanistic insights, single-cell transcriptomic and spatial mapping studies have demonstrated substantial differences between rodent and human brains in terms of cortical cell-type composition, gene expression patterns, and laminar organization [1,2]. Moreover, cross-species comparisons reveal that brain-region transcriptomic similarity is particularly limited in higher-order cognitive areas [2] that may influence injury responses and pharmacological outcomes. Neurochemical systems also differ markedly between species. Baseline levels of serotonin (5-HT), nore-

pinephrine (NE), dopamine (DA), and acetylcholine (ACh) in the prefrontal cortex vary significantly between rodents and primates [3], potentially altering drug efficacy profiles. At the gene level, the  $\mu$  opioid receptor gene (*OPRM1*) in rodents exhibits extensive alternative splicing, producing isoforms that differ from those in humans [4,5]. These isoform-specific variations can influence ligand binding, signaling bias, and therapeutic effects, thereby limiting the direct extrapolation of rodent pharmacology to human contexts. G protein-coupled receptor (GPCR) signaling adds further complexity, as ligand-directed signaling bias and  $\beta$ -arrestin-dependent pathways display species-dependent differences [6]. For the  $\mu$  opioid receptor (MOR), recruitment of  $\beta$ -arrestin and receptor trafficking are central to the ongoing debate about neuroprotection versus adverse effects such as tolerance and respiratory depression. Herkinorin, a semi-synthetic salvinorin A analog, is a MOR-



selective agonist (~8-fold specificity over  $\kappa$  opioid receptors (KOR), and ~98-fold over  $\delta$  opioid receptor) with minimal recruitment of  $\beta$ -arrestin-2 [7,8]. Its ability to induce MOR trafficking remains controversial, with some studies reporting negligible trafficking, while others suggest context-dependent trafficking [7,9]. These unique pharmacological properties make Herkinorin an ideal tool to dissect the role of MOR trafficking in hypoxic/ischemic injury.

Human induced pluripotent stem cell (iPSC)-derived neurons offer a solution to such translational challenges. These cells retain a human genetic background, express human-specific receptor isoforms, and recapitulate patient-specific molecular phenotypes, showing high concordance with post-mortem brain molecular profiles [4,10]. Our previous study showed that iPSC-derived neural cells express opioid receptors [11]. Therefore, iPSC-based neuronal models provide a physiologically relevant platform to investigate disease mechanisms and evaluate candidate therapeutics with greater translational potential.

In the current study, we hypothesized that Herkinorin exerts neuroprotective effects in human iPSC-derived neurons subjected to oxygen-glucose deprivation/reperfusion (OGD/R) by modulating MOR trafficking. To test this, we examined receptor trafficking patterns and apoptosis in iPSC-derived neurons under OGD/R, with and without Herkinorin treatment. This approach directly addresses the translational gap by combining a human-specific neuronal model with a mechanistic analysis of biased MOR agonism in hypoxic/ischemic injury.

## 2. Materials and Methods

### 2.1 Cell Lines

Human neural stem cells (NSCs) were derived from human iPSC (Cell Inspire Biotechnology, cat# iN-300, Shenzhen, China) and used between passages 2–4. The supplier certificate indicated a high-purity NSC population (>90% SOX1/NESTIN) and expansion of up to 5 passages without loss of differentiation potential. The cell identity and karyotype were verified by the vendor. The verification was performed by immunofluorescence staining, followed by microscopic counting of double SOX1 and nestin-positive cells at the second passage of the culture in at least ten randomly selected fields of view. The antibodies used were anti-SOX1 (rabbit anti-SOX1 polyclonal antibody, ab87775; 1:500, Abcam, Cambridgeshire, UK) and anti-nestin (rabbit anti-nestin polyclonal antibody, ab92391; 1:250, Abcam). Prior to induction, NSCs were tested negative for mycoplasma, and differentiation was subsequently carried out following the supplier's protocol. Briefly, NSCs were cultured in neuronal differentiation medium (08500; STEMCELL Technologies, Vancouver, BC, Canada) and seeded onto a 96-well plate coated with Poly-L-Ornithine and Laminin. The medium was replaced every 2 days for the next week. On day 8, the cells were dissociated using accutase, centrifuged, and resuspended

in neuronal maturation medium (iNM-007A, Cell Inspire Biotechnology, Shenzhen, China) to initiate the maturation process. The medium was replaced every 2 days, and on day 21 the cells were collected and identified.

### 2.2 Identification

Immunofluorescence staining was performed on neurons differentiated from NSCs to confirm neuronal identity and to visualize opioid receptor expression. Neuronal  $\beta$ -III tubulin (TUBB3) was selected as a well-established pan-neuronal cytoskeletal marker suitable for early and intermediate-stage neurons in 2–3-week cultures, allowing assessment of neurite morphology. The MOR and KOR were also stained by immunofluorescence to evaluate receptor localization, as this was relevant to the study's focus on opioid receptor trafficking. Additional late-stage neuronal or synaptic markers (e.g., Microtubule-associated protein 2 (MAP2), RBFOX3 (NeuN), synaptophysin) were not included in the current analysis due to time constraints, but are recognized as valuable for further maturation profiling and are noted as a limitation of the study. Neurons differentiated from NSCs were fixed in 4% paraformaldehyde for 20 min at room temperature. Next, cells were treated with a blocking solution consisting of Phosphate-buffered saline (PBS) containing 3% bovine serum albumin and were then permeabilized with 0.3% Triton X-100 for 30 min at room temperature. The following primary antibodies (Abcam, Cambridgeshire, UK) were diluted in the blocking solution and incubated at 4 °C overnight: anti-OPRK1 (rabbit anti- $\kappa$ -opioid receptor polyclonal antibody, ab113533; 1:1000), anti-OPRM1 (rabbit anti- $\mu$ -opioid receptor polyclonal antibody, ab10275; 1:1000), and anti-TUBB3 (mouse anti-beta-III tubulin monoclonal antibody, ab78078; 1:1000). After washing with PBS, Alexa Fluor 488-labeled secondary antibodies (cat.no. A1056 and A1089, Beyotime, Shanghai, China) were added and incubated at room temperature in a dark box for 1 h. Nuclei were labeled with 4',6-diamidino-2-phenylindole (DAPI; C1005; Beyotime). Fluorescent images were acquired on an inverted confocal laser scanning microscope using a 20 $\times$ /0.8 NA objective for overview, and a 40 $\times$ /1.2 NA water objective for high-resolution imaging.

### 2.3 Oxygen and Glucose Deprivation

To model hypoxic/ischemic cellular damage *in vitro*, we utilized a slightly modified version of previously described oxygen-glucose deprivation/reoxygenation (OGD/R) procedures [12,13]. Briefly, human iPSC-neurons were washed twice with pre-equilibrated, glucose-free Dulbecco's Modified Eagle's Medium (DMEM; Gibco, cat. no. 11966025, Thermo Fisher scientific, Eugene, OR, USA) and then transferred to a modular airtight hypoxia chamber (Billups-Rothenberg, Del Mar, CA, USA). The chamber was flushed for 15 min at a constant flow rate (20 L/min) with a certified gas mixture of 95% N<sub>2</sub>

and 5% CO<sub>2</sub>, yielding an internal oxygen tension of <1% O<sub>2</sub> as confirmed by an oxygen analyzer. The chamber was then sealed and maintained at 37 °C for an additional 2 h of OGD.

For reoxygenation, cells were returned to glucose-containing DMEM pre-equilibrated in a normoxic incubator (5% CO<sub>2</sub>, balance air; ~18–19% O<sub>2</sub>) and maintained for 24 h. pH stability was monitored using phenol red as an indicator, and the glucose concentration was restored to physiological levels (25 mM) at the start of reoxygenation. The selection of OGD and reoxygenation duration times was based on our previous systematic investigation [14].

#### *2.4 Determining the Dose-Effect Relationship and Optimal Concentration of Herkinorin for the Alleviation of OGD/R Injury in Human iPSC-Neurons*

Herkinorin (cat.no. 508018, Merck KGaA, Darmstadt, Germany) was dissolved in dimethyl sulfoxide (DMSO) to prepare a 10 mM stock solution. Working dilutions were prepared immediately before use by adding the stock directly into culture medium, ensuring the final DMSO concentration did not exceed 0.1% (v/v) in any group. Herkinorin is light-sensitive and prone to degradation. Stock solutions were therefore prepared in small batches, protected from light, and not stored for extended periods either as dry powder or dissolved in DMSO.

To determine the optimal concentration range, human iPSC-derived neurons at day 21 of differentiation were treated with Herkinorin at final concentrations of 0.05, 0.1, 0.5, 1, 10, and 50 µM for 72 h. Cell viability was assessed using the 3-(4,5-dimethylthiazol-2-yl)-2,5-diphenyltetrazolium bromide (MTT) assay. The assay was previously validated for these cells by confirming a linear relationship between absorbance and cell number, and by verifying that 0.1% DMSO alone had no measurable effect on viability. Each concentration was tested in triplicate wells in each experiment, and repeated in three independent experiments.

Based on the viability results, concentrations of 0.1, 0.5, and 1 µM were selected for subsequent OGD/R experiments. Neurons were randomly allocated into the following groups: control (vehicle only), OGD/R, OGD/R + Herkinorin 0.1 µM, OGD/R + Herkinorin 0.5 µM, OGD/R + Herkinorin 1 µM.

In the treatment groups, Herkinorin was added 24 h prior to OGD/R induction. The OGD/R procedure consisted of 2 h of oxygen-glucose deprivation followed by 24 h of reoxygenation. After treatment, the apoptosis rate was measured by Annexin V-FITC/PI flow cytometry (BD FACSDiscover™ A8 Cell, BD Biosciences, Milpitas, CA, USA), and MOR and KOR levels in membrane and cytoplasmic fractions were quantified by Western blot.

#### *2.5 Flow Cytometry*

Following treatment, apoptosis was assessed using Annexin V-FITC/PI staining (V13242, Thermo Fisher Scientific) according to the manufacturer's instructions. Data were acquired on a BD FACSCanto II cytometer and analyzed with FlowJo software v10.8 (BD Biosciences, Ashland, OR, USA).

#### *2.6 Membrane and Cytoplasmic Fractionation*

Membrane and cytoplasmic fractions were prepared using a Membrane and Cytoplasmic Protein Extraction Kit (Cat.no. KTP3005, Abbkine Scientific, Atlanta, GA, USA) containing protease/phosphatase inhibitors. Fraction purity was verified by Western blot detection of Na<sup>+</sup>/K<sup>+</sup>-ATPase and glyceraldehyde-3-phosphate dehydrogenase (GAPDH). Protein concentrations were determined by BCA assay (Cat. No. A55865, Thermo Fisher Scientific).

#### *2.7 Western Blotting*

Equal amounts of protein (15 µg) were resolved by Novex™ (4–20%) and transferred to PVDF membranes (Cat.no. XP04200BOX, Thermo Fisher Scientific). Membranes were blocked in 5% non-fat milk/TBST for 1 h at room temperature and incubated overnight at 4 °C with the following primary antibodies: anti-Caspase-3 (1:5000, ab32351, Abcam), anti-cleaved Caspase-3 (1:500, ab32042, Abcam), anti-Bax (1:2000, ab18283, Abcam), anti-Bcl-2 (1:1000, ab32124, Abcam), anti-OPRM1 (1:1000, ab10275, Abcam), or anti-OPRK1 (1:1000, ab113533, Abcam). After washing, membranes were incubated with horseradish peroxidase (HRP)-conjugated secondary antibodies for 1 h. Bands were then visualized using ECL (34580, Thermo Fisher Scientific) and imaged on a ChemiDoc XRS+ system (Bio-Rad, Hercules, CA, USA). Densitometry was performed with Image J 1.54g (Wayne Rasband and contributors, National Institutes of Health, Bethesda, MD, USA), and normalized to appropriate loading controls.

#### *2.8 Data Analysis*

Data are expressed as the mean ± standard deviation (SD). All experiments included ≥3 independent biological replicates, each with triplicate technical replicates. Data normality was assessed with the Shapiro–Wilk test. For ≥3 groups, one-way ANOVA with Tukey's post hoc test was applied for normally distributed data, and the Kruskal–Wallis with Dunn's test for non-normal data. A *p*-value < 0.05 was considered statistically significant.

### **3. Results**

#### *3.1 NSCs Differentiate Into Mature Neurons*

NSCs were induced to differentiate into mature neurons for 14–21 days. Morphological changes were moni-





**Fig. 1. Immunofluorescence staining of human iPSC-neurons.** (A) Light microscopy image of neurons. (B) Negative control showing fluorescence without primary antibody. (C) DAPI staining highlighting cell nuclei. Scale bar = 100  $\mu\text{m}$ . iPSC, induced pluripotent stem cell; DAPI, 4',6-diamidino-2-phenylindole.

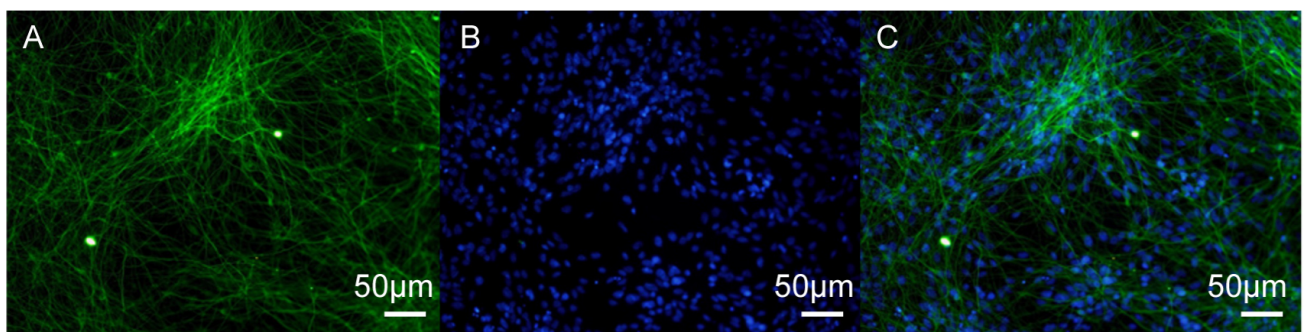


**Fig. 2. TUBB3 immunofluorescence staining in human iPSC-neurons.** (A) Neurons stained with the TUBB3 antibody, indicating beta-III tubulin. (B) Cell nuclei stained with DAPI. (C) Merged image showing co-localization of TUBB3 and DAPI. Scale bar = 50  $\mu\text{m}$ . TUBB3,  $\beta$ -III tubulin.

tored by phase-contrast microscopy, and neuronal identity was confirmed by immunofluorescence staining (Figs. 1,2). Mature neurons displayed extensive neurite outgrowths and characteristic soma morphology. Nuclei were counterstained with DAPI (blue), and neurons exhibited strong immunoreactivity for the pan-neuronal marker  $\beta$ -III tubulin (TUBB3, Fig. 2).

### 3.2 Induced Neurons Express MOR and KOR

The expression of MOR ( $\mu$  opioid receptors) and KOR ( $\kappa$  opioid receptors) in neurons 14 to 21 days post induction from NSCs was demonstrated by immunofluorescence (Figs. 3,4). These results align with our earlier research and confirm that mature neurons differentiated from NSCs are suitable for experiments investigating the neuroprotective effects of Herkinorin.

### 3.3 Effect of Herkinorin on the Viability of Human iPSC-Neurons After OGD/R

Cell viability following Herkinorin treatment was assessed by MTT assay (Fig. 5). Human neurons were incubated for 72 h with Herkinorin at 0.01, 0.05, 0.1, 0.5, 1, 10, or 50  $\mu\text{M}$ . Concentrations up to 1  $\mu\text{M}$  did not significantly reduce cell viability compared to the control, whereas 10  $\mu\text{M}$  and 50  $\mu\text{M}$  caused significant decreases in viability ( $p$

$< 0.05$  and  $p < 0.01$ , respectively). Based on these results and published data on MOR pharmacology, we chose 0.1, 0.5 and 1  $\mu\text{M}$  for subsequent experiments to ensure receptor engagement without cytotoxicity.

### 3.4 Protective Effect of Herkinorin on Human iPSC-Neurons After OGD/R

Apoptosis was quantified by Annexin V-FITC/PI flow cytometry. Representative plots (Fig. 6A–C) and the corresponding quantitative analysis (Fig. 6D) show a significant increase in apoptosis in the OGD/R group compared to the control group, which was attenuated by Herkinorin in a concentration-dependent manner (0.1  $\mu\text{M}$ : 18.2%  $\pm$  0.62%; 0.5  $\mu\text{M}$ : 16.00%  $\pm$  0.23%; 1  $\mu\text{M}$ : 13.23%  $\pm$  0.61% vs. OGD/R: 24.3%  $\pm$  0.1%,  $p < 0.01$ ). Statistical analyses were based on three independent experiments, each with triplicate measurements.

### 3.5 Effects of Herkinorin on Apoptosis-Related Protein Expression in iPSC-Neurons Under OGD/R Conditions

Western blot analysis demonstrated that OGD/R induced pronounced pro-apoptotic signaling in human iPSC-neurons (Fig. 7). Specifically, densitometric quantification revealed that OGD/R significantly increased the expression of Bax (3.65  $\pm$  0.32-fold,  $p < 0.01$ ) and cleaved Caspase-3

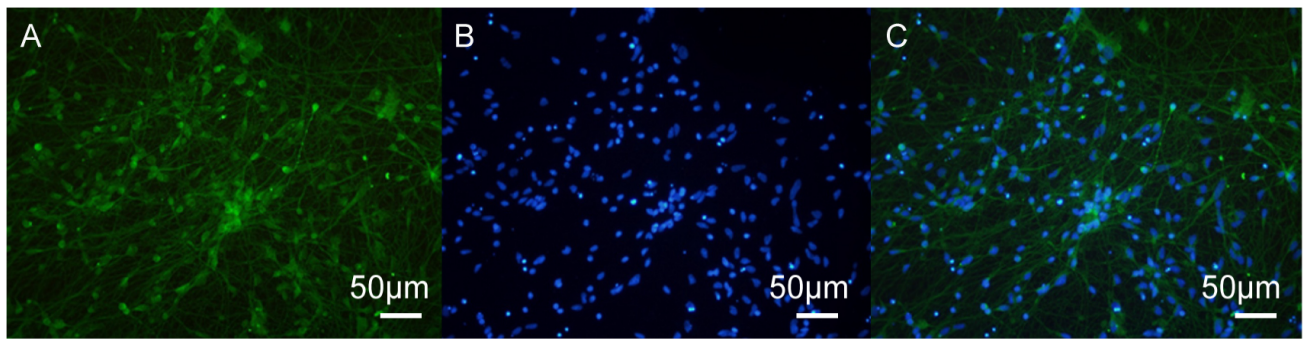


**Fig. 3. MOR immunofluorescence staining in human iPSC-neurons.** (A) Immunofluorescence image of MOR ( $\mu$  opioid receptors). (B) DAPI staining of nuclei. (C) Merged image showing co-localization of MOR and DAPI. Scale bar = 50  $\mu$ m.

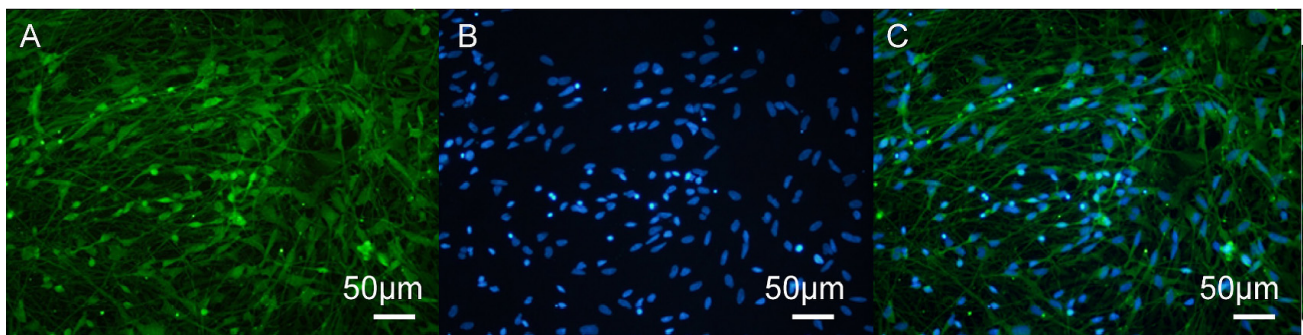


**Fig. 4. KOR immunofluorescence staining in human iPSC-neurons.** (A) Immunofluorescence image of KOR ( $\kappa$  opioid receptors). (B) DAPI staining of nuclei. (C) Merged image showing co-localization of KOR and DAPI. Scale bar = 50  $\mu$ m.

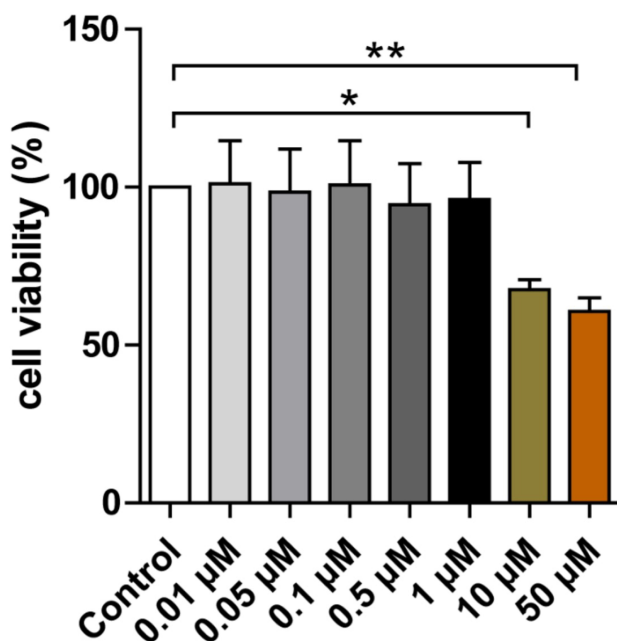


**Fig. 5. Effect of Herkinorin on the viability of human iPSC-neurons.** Treatment with 10  $\mu$ M and 50  $\mu$ M Herkinorin significantly reduced cell viability compared with the control group. Data are expressed as the mean  $\pm$  SD ( $n = 3$ ). \* $p < 0.05$ , \*\* $p < 0.01$ .

( $3.54 \pm 0.29$ -fold,  $p < 0.01$ ) relative to the control, while markedly decreasing Bcl-2 expression ( $0.48 \pm 0.04$ -fold,  $p < 0.01$ ). In contrast, total Caspase-3 expression remained unchanged across groups ( $p > 0.05$ ). Treatment with Herkinorin (1  $\mu$ M) significantly attenuated the OGD/R-induced increase in Bax ( $2.05 \pm 0.16$ -fold,  $p < 0.01$ ) and cleaved Caspase-3 ( $1.86 \pm 0.26$ -fold,  $p < 0.01$ ), while partially restoring Bcl-2 expression ( $0.89 \pm 0.08$ -fold,  $p < 0.01$  vs. OGD/R). These results indicate that Herkinorin exerts a neuroprotective effect by suppressing pro-apoptotic proteins and enhancing anti-apoptotic signaling following OGD/R injury.

### 3.6 The Effect of Herkinorin on Opioid Receptors in Human iPSC-Neurons After OGD/R

Opioid receptor trafficking was investigated by isolating membrane and cytoplasmic protein fractions. Fraction purity was validated using Na<sup>+</sup>/K<sup>+</sup>-ATPase (membrane marker) and GAPDH (cytoplasmic marker). Equal amounts of protein (15  $\mu$ g) were loaded, and all blots included molecular weight markers. Western blot analysis revealed significant changes in the distribution of  $\mu$  opioid receptor (MOR) in OGD/R group as compared to the Control group (Fig. 8A). In OGD/R neurons, cytoplasmic levels of MOR decreased significantly ( $0.49 \pm 0.04$ -fold vs. control,  $p < 0.01$ ), while membrane levels remained unchanged (Fig. 8C,E). Pre-treatment with Herkinorin increased the



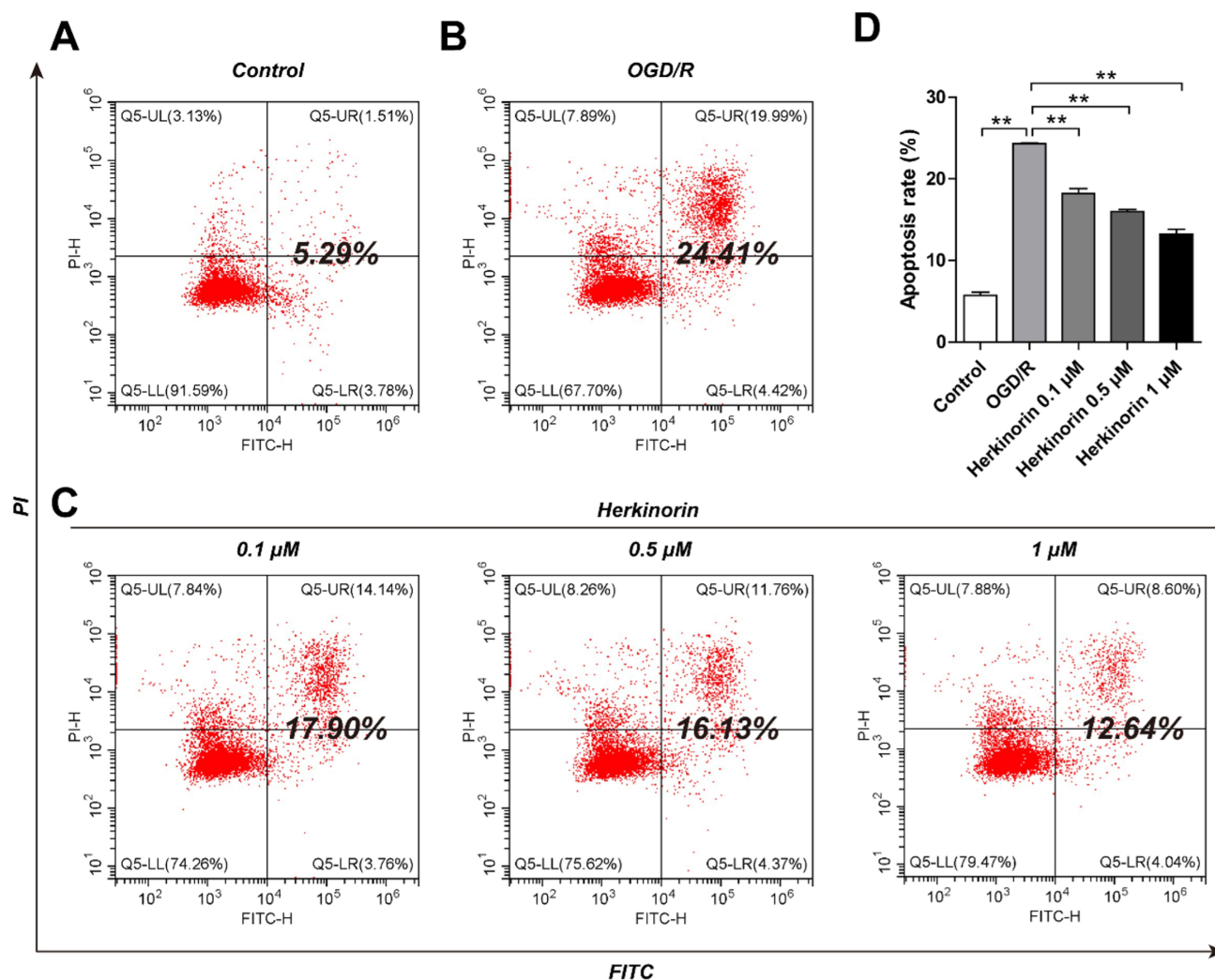


**Fig. 6. Effects of Herkinorin on apoptosis in OGD/R-treated human iPSC-neurons.** (A) Control group. (B) OGD/R group showing increased apoptosis rate. (C,D) Treatment with 0.1, 0.5, or 1  $\mu\text{M}$  Herkinorin significantly reduced apoptosis induced by OGD/R. Data are expressed as the mean  $\pm$  SD ( $n = 3$ ).  $**p < 0.01$ . OGD/R, oxygen-glucose deprivation/reperfusion. FITC, fluorescein isothiocyanate; PI, propidium iodide. FITC-H and PI-H represent fluorescence intensity in the FITC and PI channels, respectively. Q5-LL, viable cells (Annexin V<sup>-</sup>/PI<sup>-</sup>); Q5-LR, early apoptotic cells (Annexin V<sup>+</sup>/PI<sup>-</sup>); Q5-UR, late apoptotic or necrotic cells (Annexin V<sup>+</sup>/PI<sup>+</sup>); Q5-UL, necrotic cells (Annexin V<sup>-</sup>/PI<sup>+</sup>).

cytoplasmic expression of MOR (0.1  $\mu\text{M}$ :  $0.65 \pm 0.04$ -fold; 0.5  $\mu\text{M}$ :  $0.77 \pm 0.06$ -fold; 1  $\mu\text{M}$ :  $0.87 \pm 0.09$ -fold; all  $p < 0.01$  vs. OGD/R) and reduced membrane MOR at 1  $\mu\text{M}$  ( $0.56 \pm 0.05$ -fold,  $p < 0.01$ ). KOR expression was not significantly altered in either fraction under any condition (Fig. 8B,D). Data are from three independent experiments with triplicate blots.

#### 4. Discussion

Over recent decades, animal models have played a crucial role in neuroscience, particularly for *in vitro* and *in vivo* modeling of disease. These models have been instrumental in elucidating various pathophysiological events that might otherwise have remained unknown. However, the biological and genetic discrepancies between species

have been a significant barrier in the development of effective treatments for many neurological and neurodegenerative diseases. Approximately 90% of drugs that show efficacy in animal models ultimately fail in human clinical trials [15]. The utilization of human tissues, derived mainly from autopsies or fetal specimens, for cell culture models is limited by the scarcity of these resources and the challenges in scaling up primary cultures. Human iPSC-based models offer efficient platforms for elucidating pathological mechanisms and drug screening in inflammatory diseases. iPSC-derived neurons and glial cells are critical for probing the molecular mechanisms underlying hypoxic or ischemic injury and for exploring potential treatments [16,17]. The integration of human iPSC-derived brain organoids with cell culture methods to assess the effects of OGD/R is a

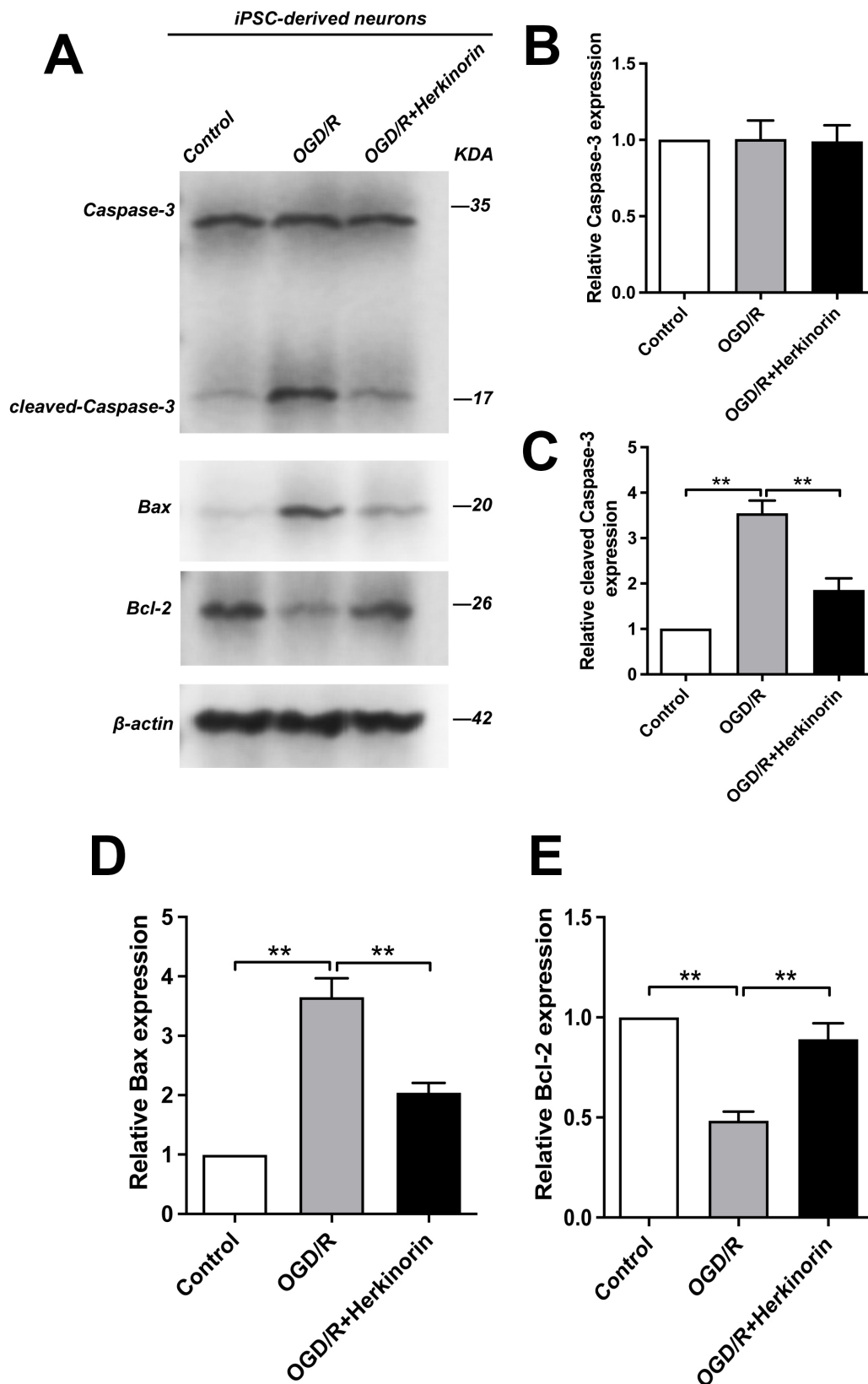


**Fig. 7.** Effects of Herkinorin on apoptosis-related protein expression under OGD/R conditions in iPSC-derived neurons. (A) Western blot analysis of Caspase-3, cleaved Caspase-3, Bax, and Bcl-2 expression in control, OGD/R, and OGD/R + Herkinorin groups. (B–E) Quantitative analysis of protein expression presented as relative fold changes: (B) Caspase-3, (C) cleaved Caspase-3, (D) Bax, and (E) Bcl-2. Data are expressed as the mean  $\pm$  SD ( $n = 3$ ). \*\* $p < 0.01$ .

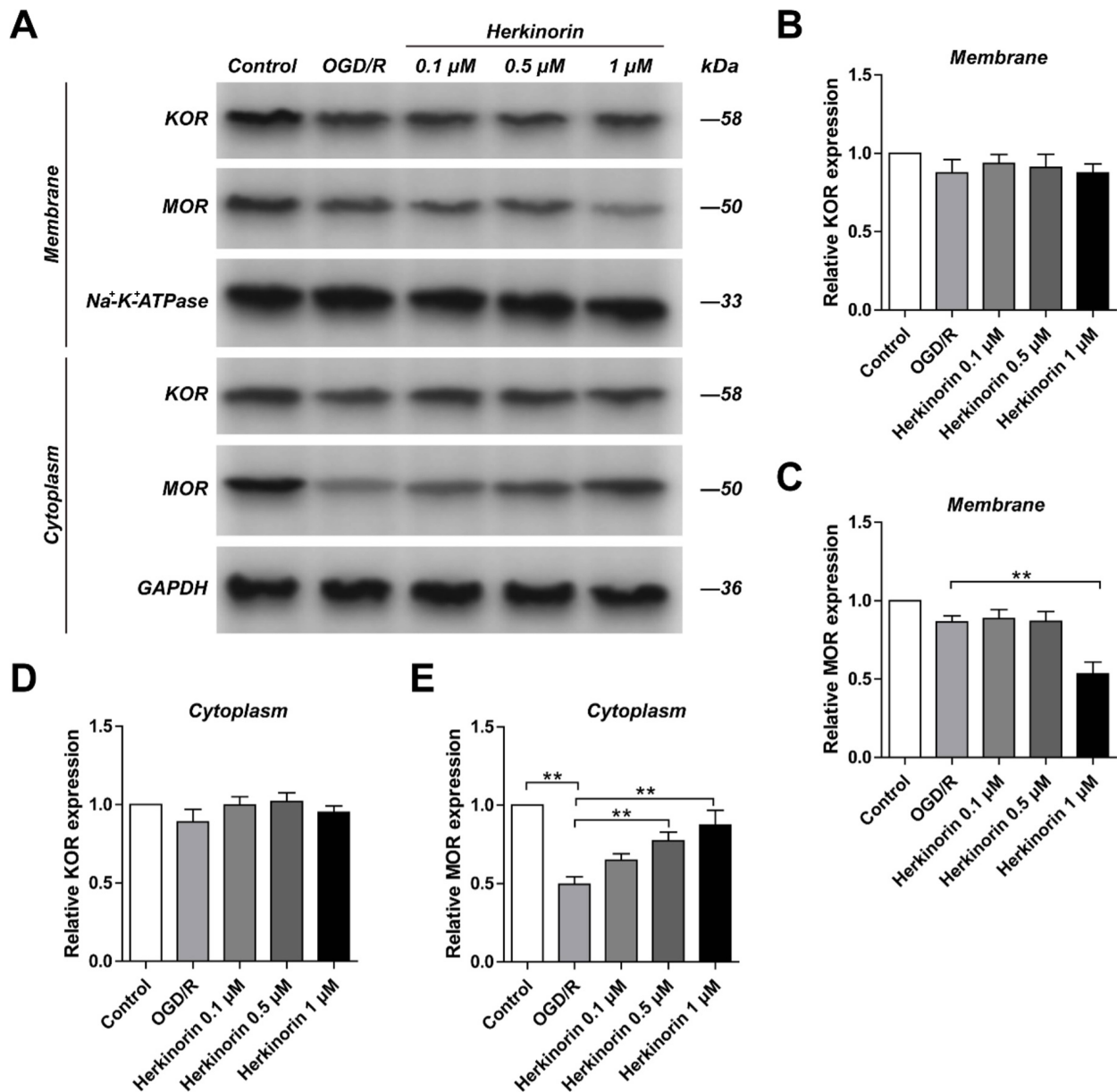


**Fig. 8. Effects of OGD/R and Herkinorin on opioid receptor expression in human iPSC-neurons.** (A) Western blot analysis of  $\mu$  opioid receptor (MOR) and  $\kappa$  opioid receptor (KOR) in membrane and cytoplasmic fractions. (B) Quantification of KOR in membrane. (C) Quantification of MOR in membrane. (D) Quantification of KOR in cytoplasm. (E) Quantification of MOR in cytoplasm. OGD/R significantly decreased cytoplasmic MOR expression compared with Control (E), while membrane MOR was unaffected (C). Treatment with 0.5 or 1  $\mu$ M Herkinorin reversed the OGD/R-induced reduction of cytoplasmic MOR (E) and decreased membrane MOR at 1  $\mu$ M (C). KOR expression showed no significant changes in either compartment (B,D). Data are expressed as the mean  $\pm$  SD ( $n = 3$ ). \*\* $p < 0.01$ .

promising approach for stroke research [18]. Luminescent neurospheres derived from human iPSCs are particularly suited for high-throughput screening aimed at discovering new treatments for acute stroke [19]. Furthermore, brain organoids based on human iPSCs serve as a novel research platform for anti-stroke drug development, and the use of iPSC-induced human cortical organoids to model OGD enables detailed investigation of the mechanisms underlying cerebral ischemia [20,21]. De Paola *et*

*al.* [21] developed a novel human 3D self-assembled iPSC-derived model (human cortical organism, hCO) to examine ischemic effects caused by OGD. These authors found that hCOs exhibited neuronal death and a reduction in neuronal network complexity after being subjected to OGD. Although OGD is commonly utilized to simulate hypoxic or ischemic injury, existing studies report considerable variability in the severity of injury [22]. Previous OGD research predominantly utilized primary rodent neuronal cells



or genetically altered cell lines in non-physiological states, such as the SH-SY5Y cell line which is known for its genetic abnormalities. Hence, there is a pressing need to develop non-neoplastic, *in vitro* human cell-based models. In 2020, Juntunen *et al.* [23] established the first *in vitro* human stroke model using neurons differentiated from human iPSCs. The lack of a standardized OGD protocol to accurately replicate hypoxic or ischemic injury *in vitro* is also noteworthy. Experimental OGD durations have varied from 1 to 24 h, sometimes followed by a reperfusion period, while oxygen levels in hypoxic conditions have ranged between 0% and 8% [23]. Our earlier study demonstrated that neurons derived from human iPSCs are capable of expressing  $\mu$ -opioid receptors [11]. Using human iPSC-derived neurons to model OGD/R, the present study assessed the effects of Herkinorin on apoptosis-related proteins and the distribution of MOR. We found that OGD/R increased the expression of pro-apoptotic Bax and cleaved Caspase-3, while decreasing that of anti-apoptotic Bcl-2. Moreover, Herkinorin at 1  $\mu$ M reversed these changes. Herkinorin was also observed to alter MOR localization, reduce membrane-associated MOR, and increase cytoplasmic MOR in a concentration-dependent manner. Our data support previous evidence that MOR activation confers neuroprotection by modulating mitochondrial apoptotic pathways [24], while extending these findings to human iPSC-derived neurons. This model has greater physiological relevance than rodent neurons or immortalized cell lines [16,17,23,25]. The Herkinorin-induced reduction in Bax and cleaved Caspase-3 expression, coupled with increased Bcl-2, suggests a shift toward an anti-apoptotic profile, consistent with MOR-mediated pro-survival signaling. In the current study we limited the experimental concentration range of Herkinorin to 0.1–1  $\mu$ M, as higher concentrations ( $\geq 10$   $\mu$ M) showed measurable cytotoxicity in preliminary MTT assays. This approach ensured that any observed neuroprotective effects were not confounded by overt toxicity. Nevertheless, it remains possible that concentrations  $>1$   $\mu$ M could elicit stronger MOR redistribution or neuroprotective effects under certain conditions. Future studies should systematically explore the 1–10  $\mu$ M range while implementing strategies to mitigate potential toxicity, such as shorter exposure durations, pulse dosing, or co-treatment with cytoprotective agents to more fully define the therapeutic window for Herkinorin in human neurons.

A notable point of contention in the literature is whether Herkinorin induces MOR internalization. While some studies have reported no  $\beta$ -arrestin recruitment or receptor trafficking [7,9], we observed a redistribution under ischemia-like conditions. Potential explanations for this discordance include differences in model systems (endogenous MOR in human neurons vs. overexpressed receptors in heterologous cells), detection methods (biochemical fractionation vs. microscopy/ $\beta$ -arrestin assays), and experimental context (hypoxia/reoxygenation vs. normoxia).

Hypoxic stress may sensitize MOR to ligand-induced internalization, with this factor being absent in normoxic studies.

The observed reciprocal changes in membrane and cytoplasmic MOR suggest internalization, which could enable protective intracellular signaling. However, we did not directly measure  $\beta$ -arrestin engagement or downstream pathways, and hence this remains speculative. Live-cell imaging and the use of pathway-specific inhibitors are needed to elucidate the exact mechanism. Limitations include the immature phenotype of iPSC-derived neurons, lack of temporal profiling of receptor trafficking, and the absence of detailed KOR analysis [26,27]. It would also be helpful to include a well-characterized MOR agonist, such as DAMGO, as a positive control for receptor trafficking and anti-apoptotic signaling. This would strengthen the mechanistic interpretation of the effects of Herkinorin by providing a benchmark for MOR-dependent responses. However, this was not feasible here due to the scope and timeline of our study. Future studies should address these gaps by incorporating mechanistic assays to validate MOR trafficking pathways.

Herkinorin, a derivative of salvinorin A and a potent agonist of MOR and KOR, may not cause the significant tolerance or dependence that is typically associated with traditional opioids. Recent research suggests that Herkinorin produces a dose-dependent, antinociceptive effect in a rat pain model, indicating its potential as a novel analgesic with a lower risk of dependence or tolerance [28]. However, research on the neuroprotective effects of Herkinorin is limited, with only a few studies hinting at such properties [14,29]. Further investigations are needed to better understand the neuroprotective capabilities of Herkinorin and the associated mechanisms. Our study revealed distinct alterations in the distribution of MOR between membrane and cytoplasmic fractions under OGD/R, particularly after Herkinorin treatment. OGD/R alone did not significantly affect membrane MOR, but 1  $\mu$ M Herkinorin reduced the membrane expression of MOR while increasing cytoplasmic levels. This reciprocal change suggests ligand-induced internalization, whereby MOR translocates from the membrane to the cytoplasm, potentially engaging protective intracellular signaling. Alternatively, OGD/R may promote cytoplasmic MOR degradation, with Herkinorin preventing this process, or enhancing redistribution. These dose-dependent effects were most pronounced at 1  $\mu$ M and warrant further investigation using live-cell trafficking assays and pathway-specific analyses. However, it is important to emphasize the narrow therapeutic window observed in our study. At concentrations above 10  $\mu$ M, Herkinorin reduced cell viability. Thus, the observed neuroprotection is confined to a limited concentration range (0.1–1  $\mu$ M), which may pose challenges for clinical translation. Overall, our results indicate that OGD/R and Herkinorin treatments lead to a redistribution of MOR between the cytoplasm and

membrane in neuronal cells. This may influence mitochondrial function and thereby affect cell survival. Conversely, some studies have found that Herkinorin does not induce  $\beta$ -arrestin recruitment or receptor trafficking [7,9]. Such discrepancies in research findings are not uncommon and may be due to differences in experimental design, methodology, conditions, and the cell lines used. Technical variations or experimental conditions could also contribute to these differences. Differences in extraction methods for membrane and cytoplasmic proteins during Western blotting may cause inconsistencies in protein recovery, thus affecting expression levels. Therefore, additional research is essential to further elucidate the mechanism of action of Herkinorin and its effects on opioid receptor trafficking. Well-designed and controlled studies are required to ensure the accuracy and reproducibility of results.

In the present study, we observed that OGD/R failed to induce detectable KOR internalization in human iPSC-derived neurons, even though MOR redistribution was evident following Herkinorin treatment. This finding may be explained by several factors. First, differences between models could play a key role. Previous observations of OGD-induced KOR internalization were mostly in rodent or immortalized neuronal cell lines (e.g., Neuro2A cells stably expressing tagged KOR) in which receptor expression levels, membrane composition, and intracellular trafficking machinery differ substantially from those of human iPSC-derived neurons [30]. Second, KOR internalization is known to require specific  $\beta$ -arrestin- and Akt-dependent signaling pathways [30,31]. The activity of these pathways under ischemia-like conditions may vary between cell types, potentially accounting for the absence of KOR trafficking in our system. Finally, the pharmacological profile of Herkinorin provides another possible explanation. Despite its structural similarity to salvinorin A (a potent KOR agonist), Herkinorin displays approximately 8-fold selectivity for MOR over KOR, with markedly reduced efficacy for KOR [32]. Such selectivity may explain the lack of detectable KOR redistribution in our OGD/R model, where MOR activation likely predominates in mediating the observed neuroprotection. Nonetheless, it remains possible that KOR contributes to protective signaling via non-internalizing, G protein-biased pathways. This warrants further investigation using KOR-selective ligands and pathway-specific assays.

## 5. Conclusions

In summary, Herkinorin reduced OGD/R-induced apoptosis and modulated MOR distribution in human iPSC-derived neurons. Future work should focus on strategies to expand its therapeutic range, such as structural modification of Herkinorin analogs, controlled delivery systems, or combination therapies designed to mitigate toxicity while preserving efficacy. These findings highlight the potential of physiologically relevant human neuronal models for

studying opioid receptor biology under ischemia-like conditions. They also underscore the need to consider experimental context when interpreting conflicting data on membrane trafficking. The future use of physiological iPSC-derived neural cells to simulate hypoxic or ischemic injury in the context of OGD should lead to further valuable insights in this field.

## Availability of Data and Materials

The datasets used and analyzed during the current study are available from the corresponding author on reasonable request.

## Author Contributions

XC and GW designed the study. ZJ, YY, and XL developed culture cells and performed immunofluorescence, flow cytometry, and Western blot analyses. Data were analyzed by ZJ and XL. The manuscript was written by ZJ and XC. All authors contributed to editorial changes in the manuscript. All authors read and approved the final manuscript. All authors have participated sufficiently in the work and agreed to be accountable for all aspects of the work.

## Ethics Approval and Consent to Participate

Not applicable.

## Acknowledgment

Not applicable.

## Funding

This work was supported by Beijing Natural Science Foundation-7212019.

## Conflict of Interest

The authors declare no conflict of interest.

## References

- [1] Hodge RD, Bakken TE, Miller JA, Smith KA, Barkan ER, Graybuck LT, *et al.* Conserved cell types with divergent features in human versus mouse cortex. *Nature*. 2019; 573: 61–68. <https://doi.org/10.1038/s41586-019-1506-7>.
- [2] Beauchamp A, Yee Y, Darwin BC, Raznahan A, Mars RB, Lerch JP. Whole-brain comparison of rodent and human brains using spatial transcriptomics. *eLife*. 2022; 11: e79418. <https://doi.org/10.7554/eLife.79418>.
- [3] Fitzgerald PJ. Neuromodulating mice and men: Are there functional species differences in neurotransmitter concentration? *Neuroscience and Biobehavioral Reviews*. 2009; 33: 1037–1041. <https://doi.org/10.1016/j.neubiorev.2009.04.003>.
- [4] Liu S, Kang WJ, Abrimian A, Xu J, Cartegni L, Majumdar S, *et al.* Alternative Pre-mRNA Splicing of the Mu Opioid Receptor Gene, *OPRM1*: Insight into Complex Mu Opioid Actions. *Biomolecules*. 2021; 11: 1525. <https://doi.org/10.3390/biom11101525>.
- [5] Grettton SK, Droney J. Splice variation of the mu-opioid receptor and its effect on the action of opioids. *British Journal of Pain*. 2014; 8: 133–138. <https://doi.org/10.1177/2049463714547115>.

- [6] Schattauer SS, Miyatake M, Shankar H, Zietz C, Levin JR, Liu-Chen LY, *et al.* Ligand directed signaling differences between rodent and human  $\kappa$ -opioid receptors. *The Journal of Biological Chemistry*. 2012; 287: 41595–41607. <https://doi.org/10.1074/jbc.M112.381368>.
- [7] Groer CE, Tidgewell K, Moyer RA, Harding WW, Rothman RB, Prisinzano TE, *et al.* An opioid agonist that does not induce mu-opioid receptor–arrestin interactions or receptor internalization. *Molecular Pharmacology*. 2007; 71: 549–557. <https://doi.org/10.1124/mol.106.028258>.
- [8] Faouzi A, Varga BR, Majumdar S. Biased Opioid Ligands. *Molecules* (Basel, Switzerland). 2020; 25: 4257. <https://doi.org/10.3390/molecules25184257>.
- [9] Tidgewell K, Groer CE, Harding WW, Lozama A, Schmidt M, Marquam A, *et al.* Herkinorin analogues with differential beta-arrestin-2 interactions. *Journal of Medicinal Chemistry*. 2008; 51: 2421–2431. <https://doi.org/10.1021/jm701162g>.
- [10] Cerneckis J, Cai H, Shi Y. Induced pluripotent stem cells (iPSCs): molecular mechanisms of induction and applications. *Signal Transduction and Targeted Therapy*. 2024; 9: 112. <https://doi.org/10.1038/s41392-024-01809-0>.
- [11] Ju ZH, Liang X, Ren YY, Shu LW, Yan YH, Cui X. Neurons derived from human-induced pluripotent stem cells express mu and kappa opioid receptors. *Neural Regeneration Research*. 2021; 16: 653–658. <https://doi.org/10.4103/1673-5374.295341>.
- [12] Liu H, Zhang Z, Xu M, Xu R, Wang Z, Di G. K6PC-5 Activates SphK1-Nrf2 Signaling to Protect Neuronal Cells from Oxygen Glucose Deprivation/Re-Oxygenation. *Cellular Physiology and Biochemistry: International Journal of Experimental Cellular Physiology, Biochemistry, and Pharmacology*. 2018; 51: 1908–1920. <https://doi.org/10.1159/000495716>.
- [13] Zhao LP, Ji C, Lu PH, Li C, Xu B, Gao H. Oxygen glucose deprivation (OGD)/re-oxygenation-induced in vitro neuronal cell death involves mitochondrial cyclophilin-D/P53 signaling axis. *Neurochemical Research*. 2013; 38: 705–713. <https://doi.org/10.1007/s11064-013-0968-5>.
- [14] Cui X, Xu X, Ju Z, Wang G, Xi C, Li J. Herkinorin negatively regulates NLRP3 inflammasome to alleviate neuronal ischemic injury through activating Mu opioid receptor and inhibiting the NF- $\kappa$ B pathway. *Journal of Cellular Biochemistry*. 2021; 9: 1085–1097. <https://doi.org/10.1002/jcb.29929>.
- [15] Drake AC. Of mice and men: what rodent models don't tell us. *Cellular & Molecular Immunology*. 2013; 10: 284–285. <https://doi.org/10.1038/cmi.2013.21>.
- [16] Duan R, Gao Y, He R, Jing L, Li Y, Gong Z, *et al.* Induced Pluripotent Stem Cells for Ischemic Stroke Treatment. *Frontiers in Neuroscience*. 2021; 15: 628663. <https://doi.org/10.3389/fnins.2021.628663>.
- [17] Liu J. Induced pluripotent stem cell-derived neural stem cells: new hope for stroke? *Stem Cell Research & Therapy*. 2013; 4: 115. <https://doi.org/10.1186/scri326>.
- [18] Iwasa N, Matsui TK, Iguchi N, Kinugawa K, Morikawa N, Sakaguchi YM, *et al.* Gene Expression Profiles of Human Cerebral Organoids Identify PPAR Pathway and PKM2 as Key Markers for Oxygen-Glucose Deprivation and Reoxygenation. *Frontiers in Cellular Neuroscience*. 2021; 15: 605030. <https://doi.org/10.3389/fncel.2021.605030>.
- [19] Van Breedam E, Nijak A, Buyle-Huybrecht T, Di Stefano J, Boeren M, Govaerts J, *et al.* Luminescent Human iPSC-Derived Neurospheroids Enable Modeling of Neurotoxicity After Oxygen-glucose Deprivation. *Neurotherapeutics: the Journal of the American Society for Experimental Neurotherapeutics*. 2022; 19: 550–569. <https://doi.org/10.1007/s13311-022-01212-z>.
- [20] Wang SN, Wang Z, Wang XY, Zhang XP, Xu TY, Miao CY. Humanized cerebral organoids-based ischemic stroke model for discovering of potential anti-stroke agents. *Acta Pharmacologica Sinica*. 2023; 44: 513–523. <https://doi.org/10.1038/s41401-022-00986-4>.
- [21] De Paola M, Pischiutta F, Comolli D, Mariani A, Kelk J, Lisi I, *et al.* Neural cortical organoids from self-assembling human iPSC as a model to investigate neurotoxicity in brain ischemia. *Journal of Cerebral Blood Flow and Metabolism: Official Journal of the International Society of Cerebral Blood Flow and Metabolism*. 2023; 43: 680–693. <https://doi.org/10.1177/0271678X231152023>.
- [22] Liu Y, Eaton ED, Wills TE, McCann SK, Antonic A, Howells DW. Human Ischaemic Cascade Studies Using SH-SY5Y Cells: a Systematic Review and Meta-Analysis. *Translational Stroke Research*. 2018; 9: 564–574. <https://doi.org/10.1007/s12975-018-0620-4>.
- [23] Juntunen M, Hagman S, Moisan A, Narkilahti S, Miettinen S. *In Vitro* Oxygen-Glucose Deprivation-Induced Stroke Models with Human Neuroblastoma Cell- and Induced Pluripotent Stem Cell-Derived Neurons. *Stem Cells International*. 2020; 2020: 8841026. <https://doi.org/10.1155/2020/8841026>.
- [24] Wang Q, Zhang L, Yuan X, Ou Y, Zhu X, Cheng Z, *et al.* The Relationship between the Bcl-2/Bax Proteins and the Mitochondria-Mediated Apoptosis Pathway in the Differentiation of Adipose-Derived Stromal Cells into Neurons. *PloS One*. 2016; 11: e0163327. <https://doi.org/10.1371/journal.pone.0163327>.
- [25] Jiang H, Ashraf GM, Liu M, Zhao K, Wang Y, Wang L, *et al.* Tilianin Ameliorates Cognitive Dysfunction and Neuronal Damage in Rats with Vascular Dementia via p-CaMKII/ERK/CREB and ox-CaMKII-Dependent MAPK/NF- $\kappa$ B Pathways. *Oxidative Medicine and Cellular Longevity*. 2021; 2021: 6673967. <https://doi.org/10.1155/2021/6673967>.
- [26] Waldhoer M, Bartlett SE, Whistler JL. Opioid receptors. *Annual Review of Biochemistry*. 2004; 73: 953–990. <https://doi.org/10.1146/annurev.biochem.73.011303.073940>.
- [27] Vaidya B, Sifat AE, Karamyan VT, Abbruscato TJ. The neuroprotective role of the brain opioid system in stroke injury. *Drug Discovery Today*. 2018; 23: 1385–1395. <https://doi.org/10.1016/j.drudis.2018.02.011>.
- [28] Lamb K, Tidgewell K, Simpson DS, Bohn LM, Prisinzano TE. Antinociceptive effects of herkinorin, a MOP receptor agonist derived from salvinorin A in the formalin test in rats: new concepts in mu opioid receptor pharmacology: from a symposium on new concepts in mu-opioid pharmacology. *Drug and Alcohol Dependence*. 2012; 121: 181–188. <https://doi.org/10.1016/j.drugalcdep.2011.10.026>.
- [29] Gui X, Cui X, Wei H, Feng G, Zhang X, He Y, *et al.* cPKC $\gamma$  membrane translocation is involved in herkinorin induced neuroprotection against cerebral ischemia/reperfusion injury in mice. *Molecular Medicine Reports*. 2017; 15: 221–227. <https://doi.org/10.3892/mmr.2016.5995>.
- [30] Xu J, Chen F, Wang S, Akins NS, Hossain MI, Zhou Y, *et al.* Kappa opioid receptors internalization is protective against oxygen-glucose deprivation through  $\beta$ -arrestin activation and Akt-mediated signaling pathway. *Neurochemistry International*. 2020; 137: 104748. <https://doi.org/10.1016/j.neuint.2020.104748>.
- [31] Xi C, Liang X, Chen C, Babazada H, Li T, Liu R. Hypoxia Induces Internalization of  $\kappa$ -Opioid Receptor. *Anesthesiology*. 2017; 126: 842–854. <https://doi.org/10.1097/ALN.0000000000001571>.
- [32] Ji F, Wang Z, Ma N, Riley J, Armstead WM, Liu R. Herkinorin dilates cerebral vessels via kappa opioid receptor and cyclic adenosine monophosphate (cAMP) in a piglet model. *Brain Research*. 2013; 1490: 95–100. <https://doi.org/10.1016/j.brainres.2012.10.024>.